February, 2012

Soft capacitive sensor for structural health monitoring of large-scale systems

Simon Laflamme, *Massachusetts Institute of Technology*
M. Kollosche
J. J. Connor, *Massachusetts Institute of Technology*
G. Kofod

JOURNAL OF STRUCTURAL CONTROL
J. Struct. Control 2010; **00**:1–21 *Prepared using* stcauth.cls *[Version: 2002/11/11 v1.00]*

Soft Capacitive Sensor for Structural Health Monitoring of Large-Scale Systems

S. Laflamme[1*], M. Kollosche[2], J. J. Connor[1], G. Kofod[2]

[1]*Department of Civil and Environmental Engineering, Massachusetts Institute of Technology, Cambridge, MA, 02139 USA*
[2]*Applied Condensed-Matter Physics, Institute of Physics and Astronomy, University of Potsdam, D-14476 Potsdam, Germany*

SUMMARY

Structural integrity of infrastructures can be preserved if damage is diagnosed, localized, and repaired in time. During the past decade, there has been a considerable effort to automate the process of structural health monitoring, which is complicated by the inherent large size of civil structures. Hence a need has arisen to develop new approaches that enable more effective health monitoring.

In this paper, a new sensing technique for damage localization on large civil structures is proposed. Specifically, changes in strain are detected using a capacitance sensor built with a soft, stretchable dielectric polymer with attached stretchable metal film electrodes. A change in strain causes a measurable change in the capacitance of the sensor, which can be directly monitored when the sensor is fixed to a structure.

The proposed method is shown here to permit an accurate detection of cracks. The proposed system deploys a layer of dielectric polymer on the surface of a structural element, and regularly monitors any change in capacitance, giving in turn information about the structural state. The smart material is composed of inexpensive silicone elastomers, which make the monitoring system a promising application for large surfaces. Results from tests conducted on small-scale specimens showed that the technology is capable of detecting cracks, and tests conducted on large-size specimens demonstrated that several sensor patches organized on a sensor sheet are capable of localizing a crack. The sensor strain also exhibits a high correlation with the loss of stiffness.

KEY WORDS: large-scale system, structural health monitoring, strain monitoring, capacitive sensor, dielectric polymer, stretchable sensor

1. Introduction

Civil infrastructures have key economical roles in societies. Their long lifespan, when combined with insufficient maintenance, increases the risks associated with failure [1]. Structural health monitoring (SHM) is expected to play a predominant role in large-scale infrastructure

*Correspondence to: E-mail: laflamme@mit.edu

Received 3 June 2010
Revised

management to ensure safety. SHM has recently attracted much attention [2], and several non-destructive evaluation strategies such as pulse-echo, dynamic response, and acoustic emission have been proposed [3]. However, due to technical or cost constraints, these methods can typically only be applied temporarily and in a localized area. Consequently, most of these methods, despite the fact that they are well understood and provide an acceptable accuracy, are difficult to implement for a large-scale structure. As a result, monitoring of civil structures is commonly done by visual inspection, which can be costly and time consuming, and depends strongly on the judgment of the inspector [4].

SHM is an integrated process consisting of sensing and data processing that leads to damage localization. The main problem for large-scale systems is to locate damage, which becomes more difficult as the number of degrees of freedom and indeterminacy increase. Some SHM techniques focus on damage localization, and usually include static sensing strategies, such as static strain gauges. These techniques are typically precise at localizing damages, but need to be deployed over the entire monitored system (analogous to a human skin) in order to be capable of complete health diagnosis. Typical complete SHM systems rapidly become economically unfeasible as the scale is increased.

Currently, sensing technology is either embedded or deployed on the surface of the monitored element. Embedded fiber optic and piezoelectric materials sensors can be efficient at damage localization. However, embedment of sensing devices is a costly process, inherently weakens the material at a certain level, and sensor replacement is almost impossible. Conversely, surface sensors have been considered. For instance, ceramic piezoelectric wafer active sensors (PWAS) can be either attached to the surface of a structure, or embedded. They permit several non-destructive evaluation methods, such as pitch-catch, pulse-echo, and phased array [5]. Thus, they can monitor the material by wave propagation similar to the conventional ultrasonic transducers. Challenges in using conventional PWAS on a surface include bonding with the monitored surface and their durability. Moreover, large areas need to be covered in order to provide sufficient information, or to increase the probability of localizing a damage that has occurred. For instance, Zou *et al.* [6] have applied an external strain sensing system to a pipeline to monitor buckling, but as in monitoring of concrete structures, point sensors are not sufficient. They used fiber optic sensors applied along the pipeline, secured externally. The disadvantage is that the bonding surface may induce impedance, thus noise [5]. Furthermore, the resolution of a fiber optic system, whether it is embedded or not, decreases as the number of cracks increases, which may lead to loss of accuracy [7].

Piezoelectric polymers have also been proposed for SHM. These can be manufactured as low-cost thin films, with a wide range of applications such as keyboards, headphones, speakers, high-frequency ultrasonic transducers [8, 9]. The most widely known PVDF sensors have been shown to be more cost-effective than strain gauges, and to require less power [10]. The performance of PVDF at high frequencies has been assessed and shown to be good at detecting damages. Zhang *et al.* [10] studied the effect at low frequencies, using patches of 19 x 5.1 mm (0.75 x 0.20 in). The design was shown to be suitable for SHM. One of the major disadvantages of PVDF, as for any surface-bonded sensing device, is that they are significantly sensitive to the quality of the bond to the applied surface due to the nature of the dynamic signal. Lin *et al.* [11] developed a fabrication technique to apply the PVDF sensor directly on the structural substrate in order to overcome the bonding issue. Other recent research using smart materials include piezoelectric paints, which are easily spreadable over an entire structure [12], and thin-film nano-PWAS composites with sensors distributed directly in the substrate, which are

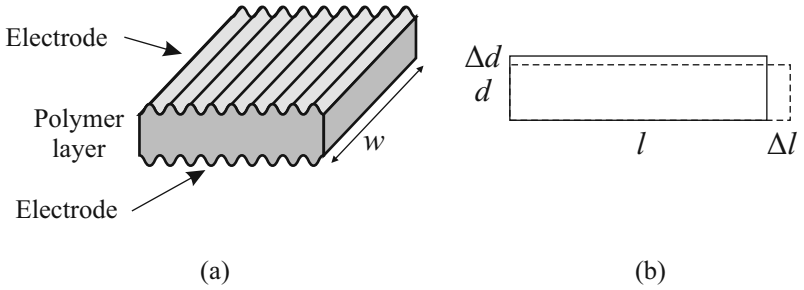

Figure 1: (a) Sketch of a capacitive unit, showing the sandwich structure of compliant corrugated electrodes surrounding an electrically insulating elastomer layer of thickness d. (b) The change in shape of the capacitive sensor due to applied compressive strain.

.

characterized by their low power requirement for pulse-echo detection of cracks [13].

In this paper, a novel monitoring technique capable of detecting changes in strain on large surfaces at low cost is presented. The sensor is a soft capacitor with a high strain sensitivity, which results in simple data processing for damage localization. Due to the simplicity of the setup, it compares well in costs to a resistance strain gauge. Furthermore, unlike dynamic strain gauges, it can be easily applied on irregular surfaces.

The paper is organized as follows: Section 2 describes the proposed monitoring technique. Section 3 discussed practical consideration in the design and application of a monitoring system using the technology. Section 4 presents the experiments conducted on small- and large-scale concrete specimens. Section 5 concludes the paper.

2. Sensor Design

In the following, a simple theory of capacitive sensing is presented, followed by a detailed description of the actual sensor used for experimental evaluations, including the constituent materials.

2.1. Theory of Capacitive Sensing

The capacitive sensor unit is modeled as a deformable capacitor, composed of two highly compliant electrodes with a surface A and separated by a constant distance d, as illustrated in Fig. 1 with corrugated electrodes. A polymer layer between the electrodes provides compliance, and the deformation characteristics of the polymer ensure large variations in the capacitance under deformations. The capacitance of a thin film capacitor C is given by:

$$C = \epsilon_r \epsilon_0 \frac{A}{d} \tag{1}$$

where ϵ_r is the relative permittivity of the polymeric medium between the electrodes, and ϵ_0 the vacuum permittivity. The deformation of the capacitor leads to a direct change in capacitance, as shown in Fig. 1(b). The length of the sensor is l and the width w.

Due to the corrugations, the width w can be assumed constant during deformation. Also, due to the incompressibility of the polymer, the length and thickness are inversely coupled. The capacitance of the sensing film, Eq. (1), can be rewritten as:

$$C_{\text{sense}} = \epsilon_r \epsilon_0 \frac{w \cdot l}{d} \tag{2}$$

A change in the capacitance may be calculated as a total differential (for small changes):

$$\Delta C_{\text{sense}} = \frac{\delta C_{\text{sense}}}{\delta l}\Delta l + \frac{\delta C_{\text{sense}}}{\delta w}\Delta w + \frac{\delta C_{\text{sense}}}{\delta d}\Delta d \tag{3}$$

where Δw vanishes. Thus, the relative change in capacitance is:

$$\Delta C_{\text{sense}} = \left(\frac{\Delta l}{l} - \frac{\Delta d}{d}\right) C_{\text{ref}} \tag{4}$$

The conservation of volume $V = l \cdot w \cdot d$ leads to the following relationship for the deformed state:

$$l \cdot w \cdot d = (l + \Delta l)(d + \Delta d)w \tag{5}$$

leading to the following relation:

$$\frac{\Delta l}{l} = -\frac{\Delta d}{d} \tag{6}$$

$\Delta l/l$ is also known as the sensor strain S. Combining Eq.'s (4) and (6), the change in capacitance with sensor strain is found to be:

$$S = \frac{\Delta C_{\text{sense}}}{2C_{\text{ref}}} \tag{7}$$

Combining Eq.'s (1) and (7) gives rise to a general expression for change in capacitance of the sensor due to a length change:

$$\frac{\Delta C_{\text{sense}}}{\Delta l} = 2\frac{\epsilon_r \epsilon_0 w}{d} \tag{8}$$

Equation (8) illustrates that the sensor sensitivity increases with sample width and inversely with sample thickness, as expected. Also, it is seen that the sensitivity may be improved by raising the permittivity of the polymer [14].

2.2. Proposed Sensor

Any stretchable polymer material with appropriate stretchable electrodes can be used to construct a stretchable capacitance sensor. Electrodes based on metal films are preferable (gold, silver, aluminium, etc.), since they have lower resistance. However, metal is commonly too stiff to be stretchable, and must therefore be prepared with a suitable microstructure. The commercially available DEAP material (Danfoss PolyPower$^{\text{TM}}$) consists of a silicone polymer (PDMS) in conjunction with a corrugated metallic compliant electrode technology [15].

The PDMS has a relative permittivity of $\epsilon_r = 3.1$ and a highly uniform film thickness $d = 80\,\mu$m, while the laminated compliant silver electrodes have a thickness of about 100

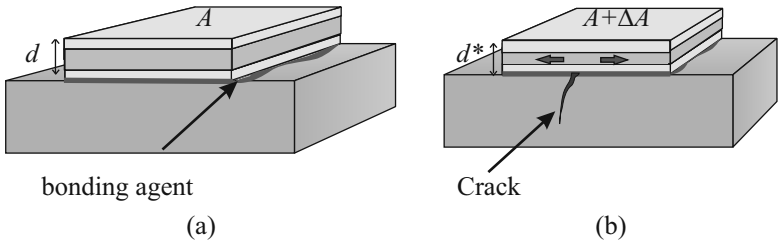

Figure 2: (a) Capacitive sensor bonded to the monitored structure; (b) local deformation resulting in a local change of the electrode area $A + \Delta A$.

nm [16]. Due to the corrugations, a uni-directional strain of about 30% strain becomes possible, much more than required for SHM of civil structures. Fig. 3 shows a roll of PolyPower$^{\text{TM}}$material.

Figure 3: Roll of PolyPower$^{\text{TM}}$material (200 mm wide).

2.3. Measurement principle

The measurement method is based on the comparison of two sensor units, a sensing capacitance C_{sense}, and a reference capacitance C_{ref}. This technique results in higher resolution during measurements, provided that both sensors have similar initial capacitances. In the comparison mode, the capacitive sensor can be compared with a capacitive sensor of any material, but in order to control for environment effects, such as temperature drift, it is preferable to compare two materials that are nominally identical. The location of the referential capacitance influences its accuracy. Here, comparison has been made between two different strategies. The first strategy entails that C_{sense} is bonded to the element under test, while C_{ref} is physically separated from C_{sense} in an arrangement termed 'non-stacked'. The second strategy, termed 'double layer' differential sensor, locates the referential capacitance directly on top of the sensing capacitance, as illustrated in Fig. 4. The use of a thick layer (approximately 500 μm) of soft glue between the layers delays the propagation of the strain to the reference capacitor C_{ref}, thus increasing the signal in the differential mode.

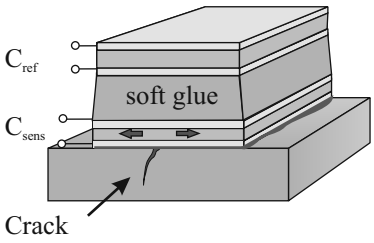

Figure 4: Sketch of a 'double layer' differential sensor separated by a soft viscoelastic glue.

3. Experimental Methods and Practical Considerations

The measurement principle behind the proposed sensor is static, while the comparable piezoelectric-based sensors are inherently dynamic sensors which compare a current sensor condition with a previous condition. For dynamic sensors, the shear lag of a bonding agent is of paramount importance, since it directly induces time delay and noise. In the case of static measurements, the influence of time delay influence is minimized by the discretization of measurements. The proposed differential sensor combines both types of measurements, by incorporating a stiff layer for direct transfer of strain to the sensor film, while the soft glue introduces a shear lag, such that the top film can serve as a mechanical memory of an earlier state.

3.1. Sensor Amplifier for Data Acquisition

The sensor must be interfaced with an amplifier to measure any changes in capacitance. The choice of amplifier also influences the level of sensitivity which can be achieved. Here, a commercially available low-cost data acquisition device was chosen, in order demonstrate the direct applicability of this technology. The particular data acquisition device (PICOAMP PSØ21, ACAM GmbH) contains the circuitry required for the differential measurement mode. All measurements presented here were obtained using this amplifier in the differential mode.

The sensitivity analysis begins by calculation of the order of magnitude of the capacitance. The largest sensor used in the experiment has a dimension of 50 x 100 mm. The capacitance of a sensor of such size can be calculated to be 3400 pF (Eq. (1)). The manual for the data acquisition device (PSØ21) indicates that for $C_{\text{ref}} = 2$ nF and a measurement frequency of 10 Hz, the smallest detectable capacitance change is $\delta(\Delta C_{\text{sense}}) = 25$ fF, which corresponds to a strain resolution of $\delta(S) = \delta(\Delta C_{\text{sense}}/2C_{\text{ref}}) = 6$ ppm. For the sensors employed here, with $l = 100$ mm, the length resolution becomes $\delta(\Delta l) = 0.4\mu$m, which is below the micrometer range and so below the possibility of any visual inspection.

3.2. Hardware Installation

Installations of most surface sensors requires the surface to be sanded, a primer applied (if necessary), and a bonding agent employed. In the present experiments, the concrete specimens had rough surfaces, onto which the sensor prototypes were installed. The concrete surfaces were manually sanded with sand paper, and an off-the-shelf concrete primer spread before the application of an off-the-shelf stiff epoxy. The sensors were manually glued on the epoxy. The

capacitance of the sensor element was measured both before and after installation and found to be identical, which is a verification that the metal electrodes were not affected by the epoxy.

This rather rudimentary installation method gave good results, demonstrating that the deployment of the sensor on the monitored structure is straightforward. Fig. 5 shows a 100 x 200 mm sheet of sensors installed on the bottom surface of a concrete beam.

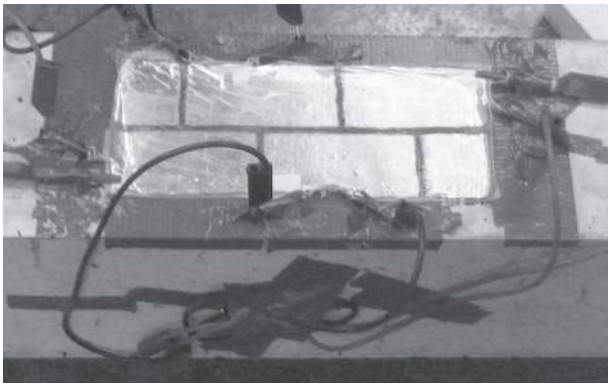

Figure 5: 100 x 200 mm sheet of sensors deployed on the surface of a concrete beam.

The connection of electrical leads to the metal electrodes was found to be challenging. This was due to difficulties in attaching stiff clamps to the soft material. A workable solution was found by reinforcing the material with a piece of tape, which also served as electrical insulation. This solution was adequate for the experiments. However, a more reliable manufacturing process is required. This should be possible with conducting inks or other soft conducting materials.

3.3. Self-Healing Property

The simplicity of the sensor translates into an improved durability. The durability can be further enhanced by enclosure of the sensor patch and hardware against influence of weather. A particular concern is material puncture or tear, which could occur during the installation procedure, or as a consequence of interaction with the surroundings (i.e. animals or vandalism). A material puncture or tear can lead to the formation of an electrically conducting path between the top and bottom electrode layers, leading to the loss of capacitive behavior. The conducting path can be removed by application of a high voltage (on the order of 10^3 volts) for a few seconds. The high voltage has the effect of burning the conducting path simply by evaporating the electrode surrounding it, thus allowing a reutilization of the unit, a property known elsewhere as 'self-healing' [15]. Fig. 6(a) shows the application of a high voltage (2.5 kV) on a unit damaged by the removal of approximately 25 mm^2 of material. Fig. 6(b) shows faint sparks during the voltage application, indicating the high current actively burning the conducting connections. Fig. 6(c) shows the material after the high voltage application. It can be observed that the circumference of the hole has been burned. The sensor was functional after the operation.

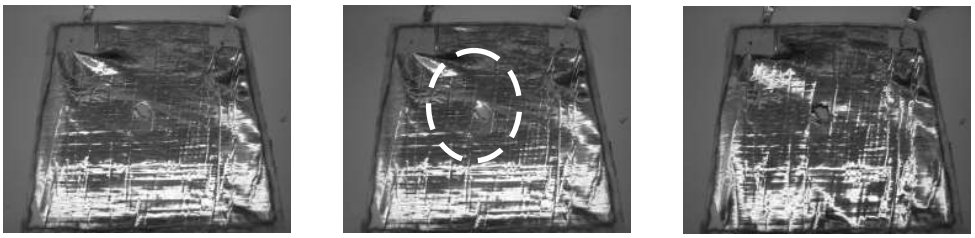

(a) (b) (c)

Figure 6: High voltage application on a damage sensor. (a) damaged sensor; (b) during the treatment with 2.5 kV; (c) after high voltage was applied and electrode in the damaged area is evaporated.

3.4. Design of Sensor Sheets

The sensor material can be cut to form several sensors arranged in different patterns, as illustrated in Fig. 5. This can also be realized by employing suitable masking during the manufacturing process of the sensor material [16]. The utilization of several sensors would lead to a more precise localization of damages. However, a small non-detecting region is introduced at each cut, denoted by the thick lines.

Patterns should be selected using judgment based on the type of damage to be localized. Here we propose a few possible patterns of sensor patches and their mode of detection, shown in Fig. 7. Fig. 7(a) is a staggered pattern, which allows for a complete coverage for flexural cracks (which would form vertically). There is redundancy in the sensors, such that two sensors will catch a single flexural crack. This is different from Fig. 7(b) where there is no redundancy in sensors. The diagonal configuration, illustrated in Fig. 7(c) would be more appropriate for the localization of shear cracks. Fig. 7(d) shows a mixture of horizontal and vertical sensors. Horizontal patches are more sensitive to curvature.

The patterned sensors allow for a further simplification in the detection scheme, by exploitation of the differential nature of the measurement technique where both C_{sense} and C_{ref} can be localized on the same sheet. Using a smart combination of patches with an appropriate electronic circuit allows damage localization by comparing several measurements within the sensor sheet using a single data acquisition device.

4. Experiments

Small-scale tests on smaller concrete specimens (beams of dimension 70 x 50 x 370 mm) were carried out to verify the measurements principle [17], while subsequent scaled-up tests (beams of dimension 200 x 150 x 1500 mm) showed that the principle would also hold in realistic settings and accurately locate cracks using patterned sheets. Fig. 8 shows the experimental setup for both tests. For the small-scale tests, two different differential sensor geometries were employed, i.e. both 'non-stacked' and 'double layer' geometries, while for the large-scale tests only the 'non-stacked' configuration was employed for technical reasons.

In both series of tests, flexural cracks are induced using a 4-point loading, and sensors placed

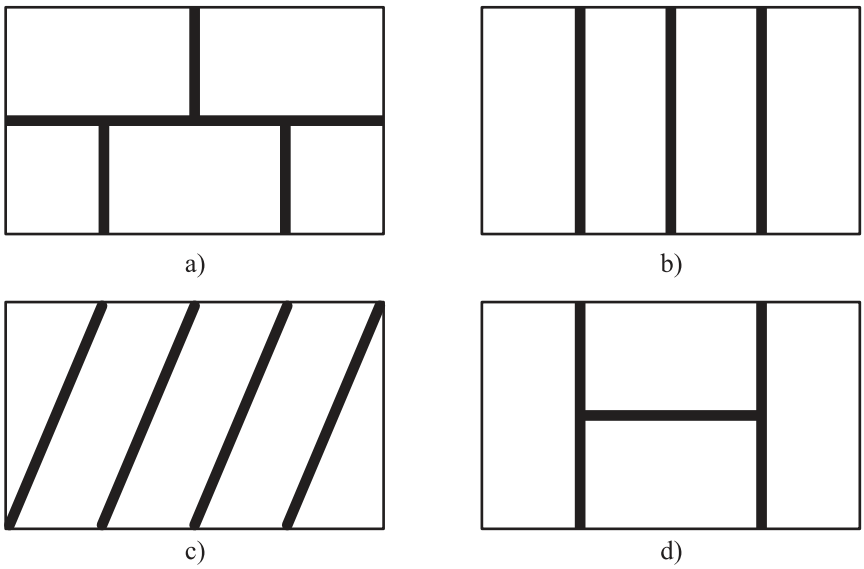

Figure 7: Different sensor patterns: (a) staggered; (b) vertical; (c) diagonal; and (d) mix horizontal-vertical.

Figure 8: Experimental setup for (a) the small-scale tests; and (b) the large-scale tests.

on the bottom of the beam to locate flexural cracks. A constant load was applied for a set period of time, and then released in order to simulate the load/no-load conditions. For the small-scale beams, the no-load condition was at the 50 N plateau, and the load was increased by 50 N increments at a loading rate of 50 N/min. The sensor dimensions were 50 x 60 mm. For the large-scale beams, the no-load condition is at the 1000 N plateau, and the load is increased by 500 N increments at a loading rate of 6000 N/min. In that case, because of the high load capacity of the beam, the no-load plateau is increased to the next 5000 N level after 20 increments. The sensor patch dimensions are 50 x 100 mm. Table I summarizes the methodologies for each series of tests. The objective of the periodic loading tests is to look at the capability of the sensor to detect cracks, where the periodic load ensures that the changes

in measurements are not a consequence of changes in curvature from an applied load.

Table I: Summary of test parameters

scale	beam size (mm x mm x mm)	sensor patch size (mm x mm)	load increment (N)	loading rate (N/min)
small	70 x 50 x 370	50 x 60	50	50
large	200 x 150 x 1500	50 x 100	500	6000

4.1. Small-Scale Tests

A high precision loading cell was used for the small-scale tests. That equipment allowed to plot displacement rates and loading rates to verify the formation of crack. A jump in those rates indicates a nonlinear displacement. The following subsections describe the results from two representative tests.

4.1.1. Mortar Specimen The first small-scale test was performed on a beam made with a low-resistance mortar (high water ratio). In this case, a 'non-stacked' configuration was employed, such that the reference sensor C_{ref} was not located on the beam. Fig. 9(a) is a plot of both sensor strain (relative change in capacitance, black curve) and displacement rate (dotted curve) against time. The shape of the dotted curve arises due to the step-wise application of load force, causing large strain rates only in short bursts. The capacitance time series shows a pronounced jump in differential capacitance (by a factor of 2) when the first crack forms. Note that there was a loss of data between the range 415 - 730 sec due to a software failure. Fig. 9(c) is a blow up of the first jump in capacitance measurement. There is a jump in the displacement rate at the same time, thus the formation of a crack. Fig.9(c) is a blow up of the region following the crack formation. The differential capacitance is sloping upwards, representing a loss in stiffness of the beam.

4.1.2. Concrete Specimen The second small-scale test is conducted on a concrete specimen. Here, a 'double layer' sensor was used (see Fig. 4). The sensor is deployed on the bottom of the concrete beam to detect flexural cracks. Fig. 10 is a graph of the sensor strain (relative change in capacitance) along with the loading rate. The loading rate is plotted instead of the displacement rate (test on mortar specimen) and exhibits clear jumps at the formation of cracks. It can be observed that the sensor is sensitive to the micro-crack formation. The micro-crack formation is deduced from the minor jump in the loading rate. The sensor also clearly detects the first crack as shown by the jumps in the capacitance measurement and the loading rate. A second crack is also detected from the measurements following a loss of stiffness.

4.2. Large-Scale Tests

Large-scale tests have been conducted to verify the correlation with the loss of elasticity and the capacity to locate cracks. The results of two representative tests are presented in this section. Both tests were made with patterned sensors, in a 'non-stack' configuration. The first test used the staggered pattern (Fig. 7(a)), and the second one used the vertical pattern (Fig. 7(c)). No

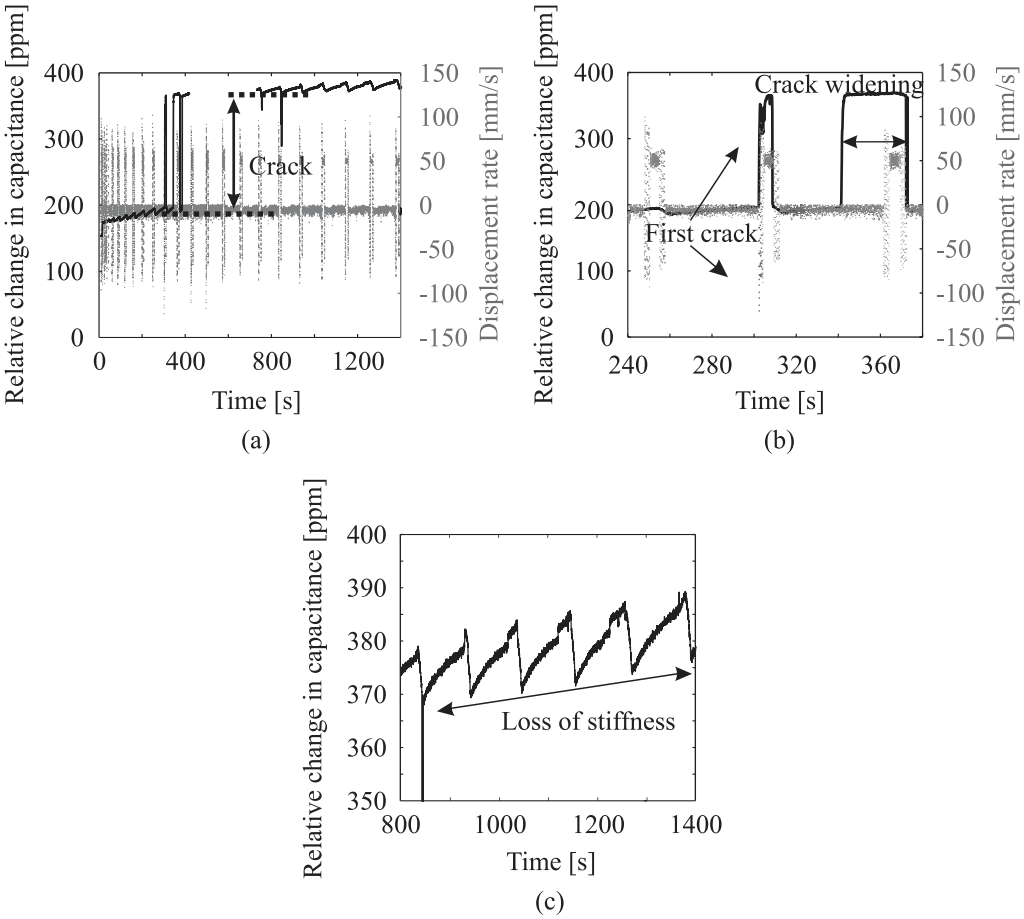

Figure 9: Differential capacitance and displacement rate against time for the small-scale test with a 'non-stacked' sensor on a mortar beam: a) time series; b) zoom on the first crack; c) zoom on the loss of stiffness.

crack formed under the sensor sheet during the first test, while a crack was visible under one of the sensor patches during the second test.

4.2.1. Staggered Pattern Fig. 5 is a picture of the sensor used for the staggered pattern test. Two data acquisition systems were used for the test. Both C_{sense} and C_{ref} were located on the same sheet. One data acquisition device was used to sense the left hand side patches, and the other was used to sense the right hand side patches. No cracks were visually detected under the patches. Fig. 11 is a plot of the relative capacitance and the relative elasticity against time. Straight lines in the relative capacitance indicate a loss of data. The correlation between both time series is 0.80. The high correlation indicates that the use of horizontal patches with a staggered pattern is capable of detecting a loss of stiffness in an element.

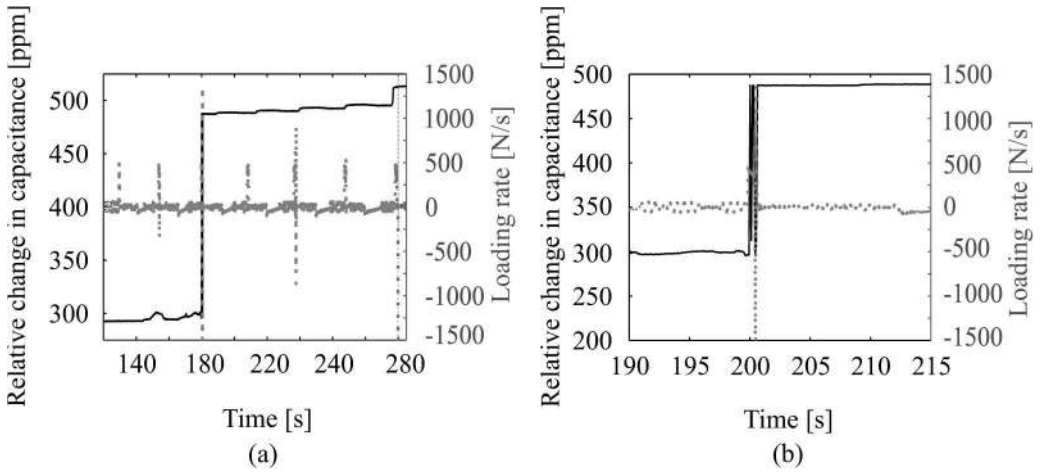

Figure 10: Differential capacitance measurement with loading rate for the small-scale test with a 'double layer' sensor on a concrete beam; (a) time-series; (b) zoom on the first crack region.

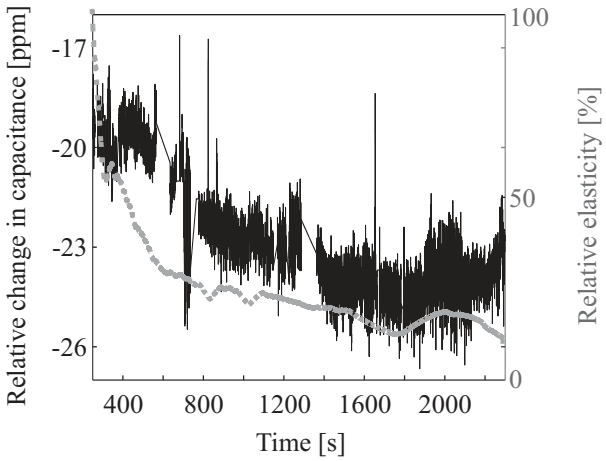

Figure 11: Relative capacitance and relative elasticity against time measured on large-scale specimen with a 'non-stacked' staggered pattern sensor.

4.2.2. Vertical Pattern Fig. 12 shows the vertical pattern sensor (Fig. 7(a)) installed on the beam (the sheet is slightly off the beam center line). Two data acquisition devices were used for the test. One acquisition device sensed the two middle patches, using one patch as C_{sense} and the other as C_{ref}. A second acquisition device employed the two end-located patches. A crack formed under one of the middle sensor patches during the experiment, and can clearly be observed in Fig. 12(b).

Fig. 13 is a plot of the relative capacitance for both sensors against time. The black line is the measurements from the two middle patches (sensor 1). Two distinct jumps in the measurements

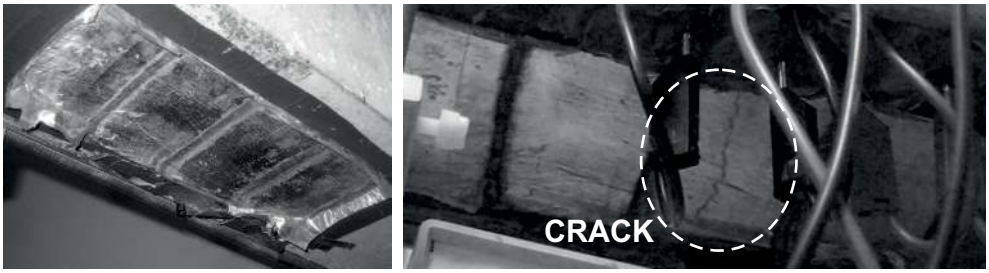

(a) (b)

Figure 12: Vertical pattern 'non-stacked' sensor sheet used for the large-scale test: (a) deployed on the beam; and (b) a crack formed under a patch.

can be seen after 5000 sec. The first jump indicates the formation of the crack. At that point, the crack was already visually observable. The second jump indicates a sudden expansion of the crack. It was visually verifiable that the size of the crack significantly increased. The dotted line is the measurements from the two end-located patches (sensor 2). No cracks located under those patches were visually tractable after the test. However, there is an important jump in the measurements slightly before 2500 sec that may indicate a crack.

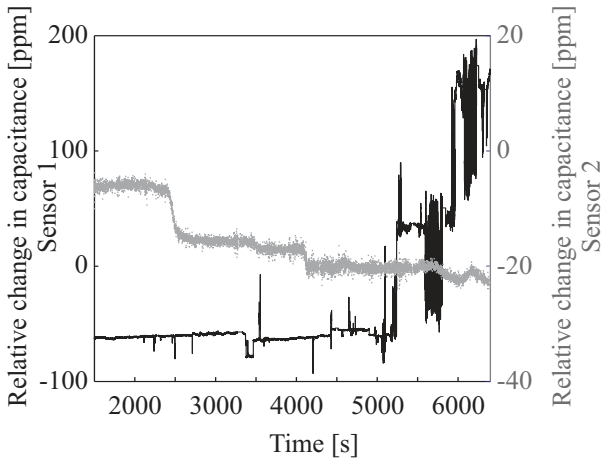

Figure 13: Relative capacitance of both 'non-stacked' sensors against time for the vertical pattern sensor experiment.

Fig. 14 is a plot of the relative capacitance of the second sensor and relative elasticity against time, similar to Fig. 14. The correlation between both time series is 0.76. The relative capacitance measurements are thus highly correlated with a loss of stiffness. The lower correlation compared to the previous test can be caused by the use of vertical patterns, which are less sensitive to changes in the beam curvature.

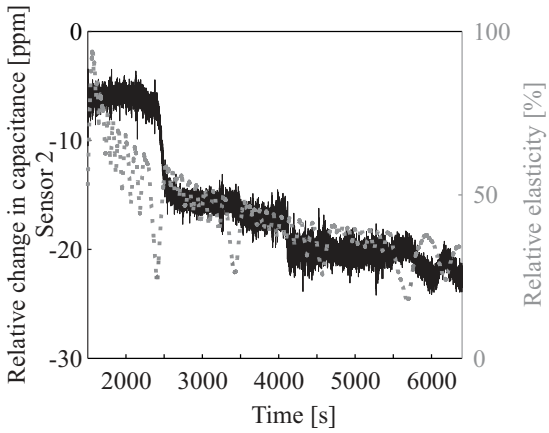

Figure 14: Relative capacitance and relative elasticity against time - 'non-stacked' sensor 2.

5. Conclusion

A new method for damage localization on large-scale structures was proposed. The new method detects changes in strain using a capacitance sensor built with a soft and stretchable dielectric polymer with attached stretchable metal film electrodes. The smart material is composed of inexpensive silicone elastomers, the acquisition sensors were low-cost commercially available devices, which makes the monitoring system a promising low-cost application for large surfaces, and easy to apply, compared to existing sensor types. Results from tests demonstrated promising performance for the proposed sensor. Tests conducted on small-scale specimens showed that the technology is capable of detecting cracks, and tests conducted on large-scale specimens demonstrated that several sensor patches organized on a sensor sheet are capable of localizing a crack. The sensor strain also exhibits a high correlation with the loss of stiffness.

6. Acknowledgments

The authors thank John T. Germaine for his priceless help and guidance during the testing process, as well as Andreas Pucher, Stephen W. Rudolph and Benjamin D. Harvatine for their valuable support with the measurement setups. MK and GK acknowledge support from the WING initiative of the Germany Ministry of Education and Research through its NanoFutur program (Grant No. NMP/03X5511).

REFERENCES

1. Karbhari VM. *Encyclopedia of structural health monitoring*, chap. Design Principles for Civil Structures. Wiley, 2009; 1467–1476.
2. Song G, Gu H, Mo Y, Hsu T, Dhonde H. Concrete structural health monitoring using embedded piezoceramic transducers. *Smart Materials and Structures* 2007; **16**:959.
3. Bungey J, Millard S. *Testing of concrete in structures*. Kluwer Academic Publishers, 1996.

4. Lynch J. Design of a wireless active sensing unit for localized structural health monitoring. *Journal of Structural Control and Health Monitoring* 2004; **12**(3-4):405–423.
5. Lin B, Giurgiutiu V, Yuan Z, Liu J, Chen C, Jiang J, Bhalla A, Guo R. Ferroelectric thin-film active sensors for structural health monitoring. *Proc. of SPIE*, vol. 6529, 2007; 65 290I.
6. Zou L, Bao X, Ravet F, Chen L, Zhou J, Zimmerman T. Prediction of pipeline buckling using distributed fiber Brillouin strain sensor. *Proc. 2nd Int. Conf. Structural Health Monitoring of Intelligent Infrastructure, Shenzhen*, 2006; 393.
7. Chen G, Sun S, Pommerenke D, Drewniak J, Greene G, McDaniel R, Belarbi A, Mu H. Crack detection of a full-scale reinforced concrete girder with a distributed cable sensor. *Smart Materials and Structures* 2005; **14**(3):88.
8. Gerhard-Multhaupt R. Less can be - more holes in polymers lead to a new paradigm of piezoelectric materials for electret transducers. *IEEE Trns. Dielectr. Electr. Insul.* 2002; **9**(5):850–859.
9. Giurgiutiu V. *Encyclopedia of structural health monitoring*, chap. Piezoelectricity Principles and Materials. Wiley, 2009; 981–991.
10. Zhang Y, Lloyd G, Wang M. Random Vibration Response Testing of PVDF Gages for Long-span Bridge Monitoring. *Proc. 4th Int. Workshop on Structural Health Monitoring, Stanford*, 2003; 115.
11. Lin B, Giurgiutiu V, Bhalla A, Chen C, Guo R, Jiang J. Thin-film active nano-PWAS for structural health monitoring. *Proc. of SPIE*, vol. 7292, 2009; 72 921M–1.
12. Zhang Y. Piezoelectric paint sensor for real-time structural health monitoring. *Proc. of SPIE*, vol. 5765, 2005; 1095.
13. Yu L, Giurgiutiu V. *Encyclopedia of structural health monitoring*, chap. Piezoelectric Wafer Active Sensors. Wiley, 2009; 1013–1027.
14. Stoyanov H, Mc Carthy D, Kollosche M, Kofod G. Dielectric properties and electric breakdown strength of a subpercolative composite of carbon black in thermoplastic copolymer. *Applied Physics Letters* 2009; **94**:232 905.
15. Benslimane M, Gravesen P, Sommer-Larsen P. Mechanical properties of dielectric elastomer actuators with smart metallic compliant electrodes. *Proc. of SPIE*, vol. 4695, 2002; 150.
16. Kiil HE, Benslimane M. Scalable industrial manufacturing of DEAP. *Proc. of SPIE*, vol. 7287, SPIE, 2009; 72 870R.
17. Laflamme S, Kollosche M, Connor JJ, Kofod G. Large-scale capacitance sensor for health monitoring of civil structures. *Proc. of 5WCSCM*, 2010.